Earth and Planetary Science Letters 449 (2016) 155–163

Contents lists available at ScienceDirect

Earth and Planetary Science Letters

www.elsevier.com/locate/epsl

# Estimating high frequency energy radiation of large earthquakes by image deconvolution back-projection

Dun Wang [a,*,1], Nozomu Takeuchi [a], Hitoshi Kawakatsu [a], Jim Mori [b]

[a] Earthquake Research Institute, University of Tokyo, 1-1-1, Yayoi, Bunkyo-ku, Tokyo, 113-0032, Japan
[b] Disaster Prevention Research Institute, Kyoto University, Uji, Kyoto 611-0011, Japan

ARTICLE INFO

*Article history:*
Received 3 February 2016
Received in revised form 27 May 2016
Accepted 28 May 2016
Available online xxxx
Editor: P. Shearer

*Keywords:*
back-projection
seismic array
high frequency energy radiation
rupture speed
supershear

ABSTRACT

High frequency energy radiation of large earthquakes is a key to evaluating shaking damage and is an important source characteristic for understanding rupture dynamics. We developed a new inversion method, Image Deconvolution Back-Projection (IDBP) to retrieve high frequency energy radiation of seismic sources by linear inversion of observed images from a back-projection approach. The observed back-projection image for multiple sources is considered as a convolution of the image of the true radiated energy and the array response for a point source. The array response that spreads energy both in space and time is evaluated by using data of a smaller reference earthquake that can be assumed to be a point source. The synthetic test of the method shows that the spatial and temporal resolution of the source is much better than that for the conventional back-projection method. We applied this new method to the 2001 $M_w$ 7.8 Kunlun earthquake using data recorded by Hi-net in Japan. The new method resolves a sharp image of the high frequency energy radiation with a significant portion of supershear rupture.



## 1. Introduction

With the recent establishment of regional dense seismic arrays (e.g., Hi-net in Japan, USArray in the North America), advanced digital data processing has enabled improvement of back-projection methods that have become popular and are widely used to track the rupture process of moderate to large earthquakes (e.g. Ishii et al., 2005; Krüger and Ohrnberger, 2005; Vallée et al., 2008; Walker and Shearer, 2009; Honda et al., 2011; Meng et al., 2011; Wang and Mori, 2011; Koper et al., 2012; Yagi et al., 2012; Yao et al., 2012; Kennett et al., 2014).

For all of these studies, time differences among seismograms recorded across regional or global arrays are used to trace the rupture migration. The methods can be classified into two groups, one using time domain analyses (Ishii et al., 2005; Krüger and Ohrnberger, 2005; Vallée et al., 2008; Walker and Shearer, 2009; Honda et al., 2011; Wang and Mori, 2011; Koper et al., 2012; Yagi et al., 2012; Yao et al., 2012), and the other frequency domain analyses (Meng et al., 2011; Yao et al., 2013). There are minor technique differences in both groups, such as the stacking methods (linear stacking, Nth-root stacking, for example, Xu et al., 2009), and the usage of cross correlation coefficients instead of stacking amplitudes (Ishii, 2011; Yagi et al., 2012). Surprisingly, all the aforementioned methods usually give consistent results, if the same datasets are used, which has been verified by the images for the March 11, 2011 Tohoku, Japan $M_w$ 9.0 earthquake.

Here we focus on the back-projection performed in the time domain using seismic waveforms recorded at teleseismic distances (30°–90°). For the standard back-projection (Ishii et al., 2005), teleseismic P waves that are recorded on vertical components of a dense seismic array are analyzed. Since seismic arrays have limited resolutions and we make several assumptions (e.g., only direct P waves at the observed waveforms, and every trace has completely identical waveform), the final images from back-projections show the stacked amplitudes (or correlation coefficients) that are often smeared in both time and space domains. Although it might not be a serious issue to reveal overall source processes for a giant seismic source such as the 2004 $M_w$ 9.0 Sumatra earthquake where the source extent is about 1400 km (Ishii et al., 2005; Krüger and Ohrnberger, 2005), it becomes a severe problem to image detailed processes of earthquakes with smaller source dimensions, such as a $M_w$ 7.5 earthquake with a source extent of 100–150 km. For smaller earthquakes, it is more difficult to resolve space distributions of the radiated energies. For the 2009 $M_w$ 6.3

* Corresponding author.
*E-mail address:* dunwang@eri.u-tokyo.ac.jp (D. Wang).
[1] Present address: State Key Laboratory of Geological Processes and Mineral Resources, School of Earth Sciences, China University of Geosciences, Wuhan 430074, China.

http://dx.doi.org/10.1016/j.epsl.2016.05.051
0012-821X/

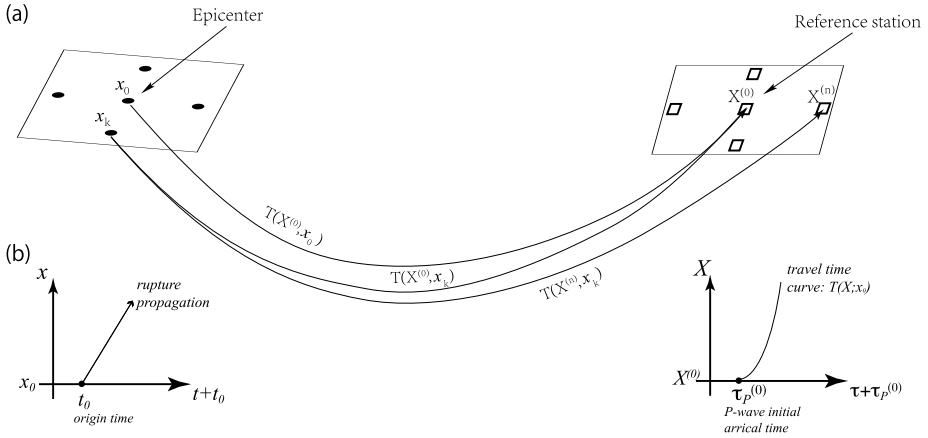


**Fig. 1.** Schematic illustrations of (a) the ray paths from the source grids to the seismic stations, and (b) the difference of time and space coordinates in source and station domains.

L'Aquila, Italy earthquake, the area of the cumulative energy shows an elliptical shape centered at the epicenter due to the large effects of the array smear (D'Amico et al., 2010).

There have been a few studies that try to improve resolution by taking the special resolution kernel (or spatial smearing) into account (Lay et al., 2009; Wang et al., 2012; Haney, 2014; He et al., 2015; Nakahara and Haney, 2015). Wang et al. (2012) deconvolved array spatial smearing that is evaluated by using the back-projection image of an aftershock, to improve the spatial resolution. Since the deconvolution was done individually for each time window, the temporal resolution was not improved. Similar ideas have been implemented for improving the spatial resolution of monitoring volcanic tremors (Haney, 2014).

In this work, we extend the idea of Wang et al. (2012) by considering the smearing both in space and time domains. It is evaluated by the spatial and temporal distribution of the back-projected image for a small earthquake that can be assumed as a point source. In this approach, the contributions of later phases (i.e. depth phases) can be taken into account, which is one of the advantages of the method in this study. Therefore this method obtains the true energy radiation of the ruptured fault, minimizing/excluding propagation effects from structures in the earth, for example, depth phases from the Earth's free surface.

## 2. Method: image deconvolution back-projection

In this study, we introduce a new inversion method, Image Deconvolution Back-Projection (IDBP), to refine the source image obtained by the sliding-window beampacking of Wang et al. (2016), which is similar to Krüger and Ohrnberger (2005). However, as our new method is applicable to more general back-projection approaches (e.g., Ishii et al., 2005), we first summarize both the conventional back projection and the sliding-window beampacking methods.

### 2.1. Conventional imaging methods

In the conventional back projection (BP), the stacked power, $\Psi^{BP}(x,t)$ for the source location $x$ and time $t$ is evaluated by

$$\Psi^{BP}(x,t)=\frac{1}{N}\int_{t-\Delta t/2}^{t+\Delta t/2}\left\{\sum_n v\left(X^{(n)},t'+t_0+T\left(X^{(n)};x\right)\right)\right\}^2 dt', \quad (1)$$

where $v$ is a certain component seismogram, $X^{(n)}$ is the location of the $n$-th station. $t_0$ is the origin time, and $T(X^{(n)};x)$ is the travel time from the source location $x$ to the station location $X^{(n)}$, $\Delta t$ is the width of the time window, and $N$ is the number of stations.

In the sliding-window beampacking, the stacked array beam power (AP), $\Psi^{AP}(x,\tau)$ is evaluated by

$$\Psi^{AP}(x,\tau)=\frac{1}{N}\int_{\tau-\Delta\tau/2}^{\tau+\Delta\tau/2}\left\{\sum_n v\left(X^{(n)},\tau'+\tau_P^{(0)}+T\left(X^{(n)};x\right)-T\left(X^{(0)};x\right)\right)\right\}^2 d\tau' \quad (2)$$

where $X^{(0)}$ is the location of the reference station, and $\tau_P^{(0)}$ is the arrival time of the initial P-phase at the reference station. A P-wave that arrives at the time $\tau+\tau_P^{(0)}$ to the reference station should arrive to a station at $X$ at time $\tau_P(X)=\tau+\tau_P^{(0)}+T(X;x)-T(X^{(0)};x)$ if the energy is radiated from a source point $x$. Fig. 1 illustrates the ray paths for travel times $T(X^{(0)};x_0)$, $T(X^{(0)};x_k)$, and $T(X^{(n)};x_k)$, as well as the coordinate system employed here: in the source side, $x_0$ and $x_k$ denote locations of the epicenter and $k$-th subevent, respectively, and in the array side, $X^{(0)}$ and $X^{(n)}$ denote locations of the reference and $n$-th stations, respectively; the superscript $^{(n)}$ generally denotes the station coordinate. In equation (2), we stack the waveform along that travel time curve to enhance the signal only when the energy indeed came from that source point. Note that the meaning of $t$ for $\Psi^{BP}(x,t)$ and $\tau$ for $\Psi^{AP}(x,\tau)$ are different, so we use different notations; the former is the source time relative to the origin time, while the latter is the P arrival time relative to the onset time in the waveform of the reference station (Fig. 1(b)). We therefore need a correction to transform $\tau$ to $t$ using the following relation:

$$t(x,\tau)=\tau+\tau_P^{(0)}-t_0-T\left(X^{(0)};x\right). \quad (3)$$

Hereafter we refer to this correction as "time correction". It can be also expressed as

$$\tau(x,t)=t+t_0+T\left(X^{(0)};x\right)-\tau_P^{(0)}. \quad (3')$$

Both of $\Psi^{BP}(x,t)$ and $\Psi^{AP}(x,\tau)$ with the time correction give similar image of the source energy radiation, and as we can see in equations (1), (2) and (3), two methods are equivalent.

In computing the image $\Psi^{AP}(x,\tau)$ by using eq. (2), we need to evaluate the following travel time:

$$\tau_P^{(0)}+\left[T\left(X^{(n)};x\right)-T\left(X^{(0)};x\right)\right]. \quad (4)$$

In this study, the arrival time $\tau_P^{(0)}$ is manually picked from the onset time of the first $P$ pulse at the reference station. In evaluating the differential travel time within the square braces, we take the